

Immobilization of Cellulase on Zinc Oxide Deposited on Zeolite Pellets for Enzymatic Saccharification of Cellulose

Tokla EOM¹, Jantiya Isanapong¹, Pisist Kumnorkaew², Krisanavej Songthanasak¹ and Peerapong Pornwongthong^{1,3,4,*}

¹ Department of Agro-Industrial, Food and Environmental Technology, Faculty of Applied Science, King Mongkut's University of Technology North Bangkok, Bangkok, Thailand

² Innovative Nanocoating Research Team, National Nanotechnology Center, National Science and Technology Development Agency, Pathum Thani, Thailand

³ Food and Agro-Industry Research Center, King Mongkut's University of Technology North Bangkok, Bangkok, Thailand

⁴ Agritech and Innovation Center, King Mongkut's University of Technology North Bangkok Techno Park, Bangkok, Thailand

Abstract. The consumption of fossil fuels to fulfill the global energy demand can cause global warming issues. Renewable energy, i.e., bioethanol, from lignocellulosic biomass, is a promising source of alternative energy to fossil fuels. The conversion of lignocellulosic biomass into bioethanol requires the release of fermentable sugars during the saccharification process using cellulase. However, the utilization of this enzyme on an industrial scale is not feasible due to its difficult separation, instability, and high cost. Here, we present a method for cellulase immobilization on functionalized zinc oxide prepared from either zinc nitrate hexahydrate (ZnO(I)) or zinc acetate dihydrate (ZnO(II)) solutions on zeolite (ZEO) pellets. The immobilized cellulase on ZnO-ZEO structures was characterized by scanning electron microscopy, X-ray diffraction spectroscopy, and Fourier transform infrared spectroscopy. The immobilization efficiencies of immobilized cellulase either on ZnO(I)-ZEO or ZnO(II)-ZEO were determined as $58.17 \pm 0.75\%$ and $55.51 \pm 0.81\%$, respectively. The immobilized cellulase on ZnO-ZEO was capable of catalyzing microcrystalline cellulose breakdown, releasing reducing sugars. The immobilized cellulase on these structures could be recycled up to four repetitive runs. Based on kinetic data, both the Michaelis constants (K_m) and maximum reaction velocity (V_{max}) of the immobilized cellulase on the ZnO-ZEO structures were lower than those of free cellulase. This suggests that immobilized cellulase has a higher affinity toward the substrate, but a lower reaction rate than the free enzyme.

Keywords. Biocatalysis, Enzymatic hydrolysis, Enzyme kinetics, Reusability

1 Introduction

Environmental concerns about oil supply shortages have encouraged researchers to develop innovative and cost-effective technologies for the effective production of renewable energy, including biodiesel, biohydrogen, biobutanol, bioethanol, and biomethane [1,2]. These alternative and environmentally friendly fuels are usually produced from lignocellulosic biomass, which is widely distributed throughout the world [3]. Lignocellulosic biomass is typically composed of 40-60% cellulose, 20-30% hemicellulose, and 15-20% lignin. It is considered the most abundant material for the generation of biobased fuels and value-added chemicals [4-7]. Additionally, the utilization of lignocellulosic biomass for the production of these products can reduce open combustion, mitigating global warming [4,8].

In the process of lignocellulosic biomass conversion, a hydrolysis step is required to break the long-chain polysaccharides, especially cellulose, in the biomass into a simple monosaccharide (sugar). Chemical, physical, and biological techniques have been applied for the hydrolysis of polysaccharide structures in biomass [9-11]. Both chemical and physical technologies

are frequently operated using strong acids at high temperatures and pressure. Under these extreme conditions, the process not only generates fermentable sugars, but also undesired products, which require further purification. On the other hand, enzymatic saccharification of cellulose is commonly used in industries for fermentable sugar production due to its mild hydrolysis conditions, high efficiency, and high specificity [9,12]. However, the saccharification process requires the use of hydrolytic enzymes to catalyze the breakdown of cellulose structures.

Cellulases are hydrolytic enzymes used in various industries, including animal feed, bioenergy, food, textile, agriculture, and so on [13,14]. Cellulase is considered a key enzyme for decomposing the long-chain structural carbohydrates of biomass into simple reducing sugars. However, the direct application of cellulase as a catalyst for achieving an efficient hydrolyzing cellulose substrate can be an expensive process because of its limited recovery and reuse [13,15]. This causes impurity of the products due to the cellulase remaining in the enzymatic hydrolysate [16]. To overcome this drawback, the immobilization of cellulase is one of the most powerful and simple

* Corresponding author: peerapong.p@sci.kmutnb.ac.th

techniques for making the process stable, recyclable, and cost-effective [16-18]. Immobilization can be conducted using various approaches, including covalent binding, encapsulation, entrapment, physical absorption, and cross-linked aggregates [19].

Covalent binding is considered to have the most potential, and provides reliable results due to the strong interaction between the enzyme and the support material, leading to difficulty in the carrier dissociating from the enzyme [20]. Also, the stability of the covalent bond allows immobilized cellulase to be reused a number of times, meaning the covalent bond process has attracted much attention at an industrial level [21]. The factor affecting the covalent binding in immobilization is the surface-functionalization and cross-linking that connects an active group of the support with the enzyme. Zhang *et al.*, [21] reported that 3-aminopropyltriethoxysilane (APTES) is an essential reagent used to modify the support surface and form an active amino group, while glutaraldehyde (GA) plays the role of a cross-linker that binds between the functional group of the support and the cellulase [21, 22]. Choosing a support is an important step in the process of cellulase immobilization; thus, physical strength, chemical stability, and cost-effectiveness are the preferred characteristics of an immobilized support [21].

Many studies have immobilized cellulase on various types of supports, including functionalized magnetic Fe₂O₃/Fe₃O₄ nanocomposites [22], sodium alginate-polyethylene glycol-chitosan [16], magnetic gold mesoporous silica nanoparticles core shell [23], magnetic nanoparticles [24], metal-organic frameworks [25], and hydrogel microspheres [26]. Recently, researchers have reported on glucose oxidase immobilized on zinc oxide nanowires [27], laccase immobilized on a zinc oxide nanoarray [28], a chitinolytic enzyme immobilized on a polyurethane/nano ZnO matrix [29], and glucose oxidase immobilized on zinc oxide nanoparticles [30].

Among these supports, zinc oxide (ZnO) nanoarrays have attracted much attention due to their specific benefits compared to other nanometal oxides, including a large specific surface area, great biocompatibility, nontoxicity, stabilized properties, and low cost [28, 31, 32]. ZnO has a variety of structures such as nanoparticles, nanotubes, nanowires, nanorods, and nanoflowers; these structural variations can provide large specific surface areas with potential applications in several specific fields of nanotechnology [31]. Immobilization of α -amylase on nano ZnO [32] and laccase on a ZnO nanoarray [28] has been reported. Interestingly, no report on the application of ZnO as a support for the immobilization of cellulase was found in the literature review, although a number of other types of supports have been successfully synthesized and applied for the immobilization of cellulase [33,34].

This study aims to develop a novel strategy for cellulase immobilization on functionalized ZnO deposited on spherical zeolite (ZnO-ZEO). The biocatalysis of immobilized cellulase was evaluated by hydrolyzing microcrystalline cellulose (MCC) to release simple fermentable sugars. The kinetic reaction of free

and immobilized cellulase was experimentally compared using a series of MCC concentrations as the substrate, and the Michaelis-Menten constant (K_m) and maximum velocity (V_{max}) were determined from the Lineweaver-Burk plot. Furthermore, the reusability of the immobilized cellulase was also investigated.

2 Materials and methods

2.1 Materials

Reagents such as APTES (98%), GA (50% in H₂O), and cellulase (enzyme blend) were purchased from Sigma-Aldrich (Saint Louis, MO, USA). MCC and 3,5-dinitrosalicylic acid (DNS; 98%) were obtained from Loba Chemie Pvt Ltd. (Mumbai, India); zinc nitrate hexahydrate, zinc acetate dihydrate, citric acid monohydrate, and sodium hydroxide pellets were procured from Kemaus (NSW, Australia). Commercial ZEO in spherical pellets (ZEO-4A, size 1.7-2.5 mm, 99.9% purity) was bought from Zibo Yinghe Chemical Co., Ltd. (Shandong, China).

2.2 Fabrication of ZnO on ZEO pellets

Commercial ZEO pellets were used as a support for zinc oxide deposition. Briefly, 7 g of zinc nitrate hexahydrate (ZNH) and zinc acetate dihydrate (ZAD) were separately dissolved in 30 ml of distilled water with constant stirring until clear and homogenous solutions were obtained. Then, 20 g of ultrasonically cleaned (in isopropanol and deionized water for 15 min each) ZEO were added into both prepared Zn²⁺ solutions (solution ZNH \rightarrow ZnO(I) and ZAD \rightarrow ZnO(II)); they were then incubated at 50 °C for 2 h. The products were then cooled to room temperature and aged overnight. The obtained ZnO(I)-ZEO and ZnO(II)-ZEO were dried at 105 °C for 1 h and calcinated at 350 °C for 30 min.

2.3 Surface modification of ZnO-ZEO

The surface of the ZnO-ZEO was modified by APTES and glutaraldehyde, as reported by Isanapong and Pornwongthong [28]. Briefly, 15 ml of freshly prepared 2% (v/v) 3-APTES in acetone was added to 10 g of ZnO(I)-ZEO and ZnO(II)-ZEO and then incubated at 50 °C while being stirred at 150 rpm. Upon completion of the reaction, the obtained APTES-ZnO(I)-ZEO and APTES-ZnO(II)-ZEO were washed several times with acetone and deionized water to remove the unbounded APTES. Then, the obtained APTES-ZnO-ZEO supports were placed into 15 ml of 5% GA in a sodium phosphate buffer (0.1 M, pH 7.4) at room temperature. After aging for 4 h, the obtained functionalized ZnO-ZEO supports were washed with a sodium phosphate buffer solution to clean the unbounded GA. The obtained functionalized ZnO-ZEO supports were dried at 105 °C for 30 min and were finally kept at room temperature before being used in the immobilization of cellulase.

2.4 Immobilization of cellulase

Briefly, 5 g of each functionalized ZnO-ZEO support was soaked in 30 ml of 50% cellulase solution in a sodium citrate buffer (0.05 M, pH 5.0). The mixture was reacted at 22 °C overnight under constant shaking at 120 rpm. Cellulase was immobilized on each functionalized ZnO-ZEO support by covalent binding. Finally, the immobilized cellulase on ZnO-ZEO was obtained simply via filtration. The immobilized cellulase on ZnO-ZEO was further washed with 5 ml of sodium citrate buffer two times to remove noncovalently attached cellulase. The supernatant and washing solution were used to determine the protein by the Lowry method [35], and bovine serum albumin (BSA) was used as the standard. The absorption was read at 750 nm. Binding efficiency and immobilization efficiency were calculated according to Eq. (1) and (2) [24],

$$\text{Binding efficiency (\%)} = (\text{Total protein bound} / \text{Total protein added}) \times 100 \quad (1)$$

$$\text{Immobilization efficiency (\%)} = [(C_i - C_s) / C_i] \times 100 \quad (2)$$

where C_i and C_s are the initial cellulase concentration and cellulase concentration in the supernatant after immobilization, respectively. The immobilized cellulase on ZnO-ZEO was further confirmed by Fourier transform infrared (FTIR) spectroscopy. Additionally, the immobilized enzyme was also characterized by X-ray diffraction (XRD) and scanning electron microscopy (SEM).

2.5 Stability of immobilized cellulase at different pH values and temperatures

The effect of different pH values (3, 4, 5, 6, 7, and 8) on the biocatalytic activities of free and immobilized cellulase, prior to MCC hydrolysis, was investigated using a sodium citrate buffer and heating at 50 °C for 1 h in a water bath without shaking. The effect of temperature was evaluated at various temperatures (30, 40, 50, 60, and 70 °C) at pH 5.0 while being incubated in a water bath without shaking. The residual biocatalytic activities of cellulase at different pH values and temperatures were determined; pH 5.0 and 50 °C were considered the reference for determining the relative biocatalytic activity of free and immobilized cellulase.

2.6 Estimation of enzyme kinetics

The enzyme kinetics of free and immobilized cellulase were experimentally compared in this study. Hydrolysis reaction assays using either free cellulase (2.99 Filter paper unit (FPU)/g MCC) or 3 pieces of immobilized cellulase on ZnO-ZEO in triplicate were performed at 50 °C with constant stirring (150 rpm) for 48 h using MCC as the substrate to calculate the cellulase biocatalytic

activity. A series of substrate concentrations were prepared from 0.05 to 0.30 mg/ml in a sodium citrate buffer (0.05 M, pH 5). A Lineweaver-Burk plot was used to estimate the Michaelis-Menten constant (K_m) and maximum velocity (V_{max}) of free and immobilized cellulases.

2.7 Reusability assay

The recovery and recycling stability of the immobilized cellulase were determined by employing MCC as the raw material. Briefly, free cellulase (6.5 FPU/g MCC) and 12 pieces of immobilized cellulase on ZnO-ZEO were experimentally compared by hydrolyzing 2% (w/v) MCC at 50 °C with constant stirring (150 rpm). After one batch of hydrolysis, the immobilized cellulase was collected by simple filtration, washed several times with distilled water, and reused in the subsequent batch of hydrolysis. The hydrolysis was experimentally repeated for up to four cycles. The enzymatic activity was considered as 100% for the original activity at the first cycle, and the activities in subsequent batches of hydrolysis were determined relative to the first cycle. In this work, all experiments were conducted in triplicate and the average value is reported.

2.8 Statistical analysis

The obtained data were statistically compared using analysis of variance (ANOVA) through a post hoc t-test. A pair was considered statistically significant when the p -value was less than 0.05.

3 Results and discussion

3.1 Characterization of immobilized cellulase on ZnO-ZEO

ZnO particles were successfully deposited on the ZEO pellets. According to the SEM images, the particle size of the ZnO on the surface of the ZEO samples appears to increase with a large aggregate, making it difficult to determine the particle size (Figure 1(a) and 1(b)). It was found the morphology of ZnO did not alter after the immobilization of cellulase (Figure 1(c) and 1(d)). From this observation, it is impossible to illustrate the presence of the immobilized cellulase on ZnO-ZEO structures. This may be due to a very small amount of enzyme.

In this study, an X-ray diffractometer in plane mode was employed to characterize the crystal structure of the ZnO on the surface of the ZEO. Figure 2 depicts the XRD patterns of ZnO, ZnO(I)-ZEO, ZnO(II)-ZEO, immobilized cellulase on ZnO(I)-ZEO, and immobilized cellulase on ZnO(II)-ZEO. Based on the standard XRD pattern of ZnO, it was found that the XRD pattern of all ZnO samples matched well with the hexagonal ZnO wurtzite (ICSD Collection Code: 290,322). This finding

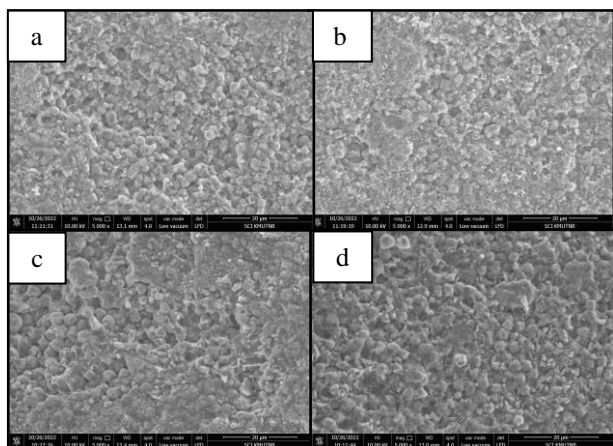


Fig. 1. SEM images of (a) ZnO(I)-ZEO, (b) ZnO(II)-ZEO, (c) immobilized cellulase on ZnO(I)-ZEO, and (d) immobilized cellulase on ZnO(II)-ZEO

is in good agreement with Isanapong and Pornwongthong's study [28]. Therefore, the XRD pattern confirmed the presence of spherical ZnO on the surface of the ZEO pellets. The XRD patterns also exhibited a slight decrease in the intensity of the diffraction peak after the immobilization of cellulase on the ZnO-ZEO support. This reduction could possibly exist during the two successive processes, i.e. surface modification and immobilization. Note that the diffraction peaks starting from 10° to 30° result from the ZEO pellets.

To acquire more information, FTIR analysis of ZnO(I)-ZEO, ZnO(II)-ZEO, immobilized cellulase on ZnO(I)-ZEO, immobilized cellulase on ZnO(II)-ZEO, and free cellulase was conducted. As illustrated in Figure 3, the FTIR spectra of the ZnO-ZEO supports display the characteristic bands of a hydroxyl group at 3445 cm^{-1} and 1654 cm^{-1} . These bands were involved in the stretching and bending vibrations of the OH groups, resulting from the presence of absorbed water [32]. The vibrational band observed in the range of 674 cm^{-1} and 554 cm^{-1} represents the stretching mode of the Zn-O bond [28,29]. In the case of the immobilization of cellulase, no additional peak was observed. The FTIR spectra of immobilized cellulase on ZnO(I)-ZEO and immobilized cellulase on ZnO(II)-ZEO were similar to those of the ZnO(I)-ZEO and ZnO(II)-ZEO supports. It was observed that the peak intensity dramatically decreased at around 1652 cm^{-1} in the immobilized cellulase on ZnO(I)-ZEO and immobilized cellulase on ZnO(II)-ZEO compared to the ZnO(I)-ZEO and ZnO(II)-ZEO supports. This finding was attributed to a decrease in the amide bond from the attached cellulase to the ZnO-ZEO supports.

In addition, the binding efficiency and immobilization efficiency were investigated using BSA as the standard and were measured at 750 nm . The immobilization efficiency was found to be $58.57 \pm 0.75\%$ and $55.51 \pm 0.81\%$ for immobilized cellulase on ZnO(I)-ZEO and immobilized cellulase on ZnO(II)-ZEO, respectively, indicating a medium binding efficiency. Therefore, the surface of the ZnO-ZEO support was not completely covered by cellulase, and the

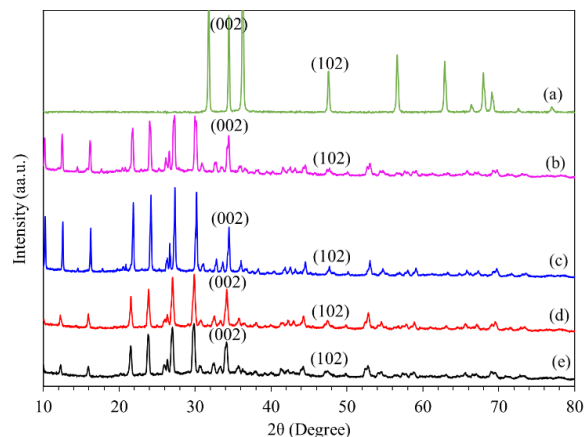


Fig. 2. XRD patterns of (a) ZnO, (b) ZnO(I)-ZEO, (c) ZnO(II)-ZEO, (d) immobilized cellulase on ZnO(I)-ZEO, and (e) immobilized cellulase on ZnO(II)-ZEO.

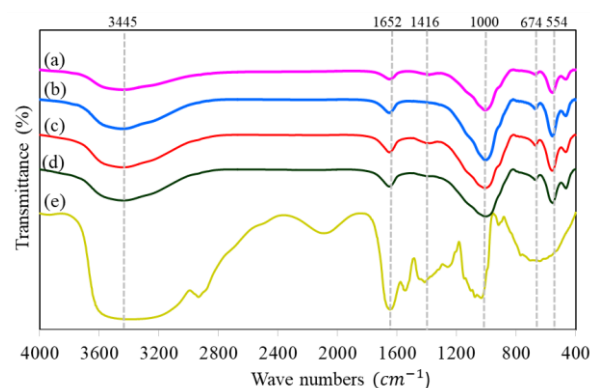


Fig. 3. FTIR spectra of (a) ZnO(I)-ZEO, (b) ZnO(II)-ZEO, (c) immobilized cellulase on ZnO(I)-ZEO, (d) immobilized cellulase on ZnO(II)-ZEO, and (e) free cellulase.

obtained results agree well with the SEM, XRD, and FTIR results. This study suggests that ZnO-ZEO can be considered as an alternative support for the effective immobilization of cellulase.

3.2 Biocatalytic activity assay

The biocatalytic activity of free and immobilized cellulase was experimentally compared by hydrolyzing the MCC substrate to release fermentable sugars. The effect of different pH values and temperatures on the hydrolysis was also investigated, as these two main factors affect the molecular structure of enzymes and cause their biocatalytic activity to decrease [17,32]. First, the effect of different pH values ranging from 3 to 7 on the hydrolysis reactions at 50°C for 1 h was studied, and the results are presented in Figure 4(a). Both free and immobilized cellulase showed the maximum biocatalytic activity at pH 5. It was noted that immobilized cellulase showed low activity in the pH range from 6 to 7 compared to free cellulase. On the other hand, when the hydrolyzed solution's pH value was 8, the biocatalytic activity of immobilized cellulase

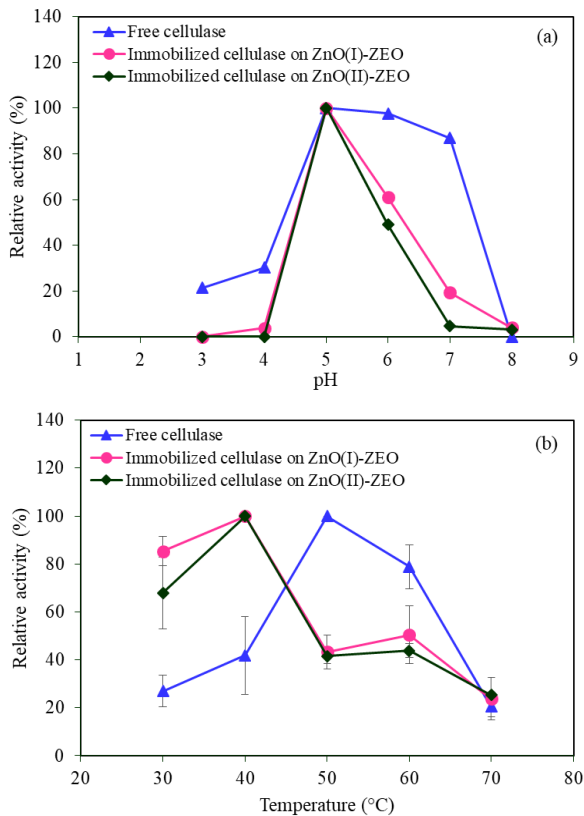


Fig. 4. Effect of hydrolysis pH (a) and hydrolysis temperature (b) on the immobilized cellulases and free cellulase.

on ZnO(I)-ZEO and immobilized cellulase on ZnO(II)-ZEO retained 3.90% and 3.05%, respectively, while that of free cellulase was absent. Hence, the immobilization process ineffectively protected the cellulase from the severe acidic and alkaline hydrolysis media. Moreover, the isoelectric point of cellulase was 4.8 and ZnO was about 9.5 [32]. This could be attributed to the wide range of instability of cellulase and the supports, thereby resulting in less resistance of immobilized cellulase toward pH change compared to the free enzyme.

The effect of different temperatures ranging from 30 °C to 70 °C on the biocatalytic activity of free and immobilized cellulase was also assessed at pH 5. As illustrated in Figure 4(b), the temperature strongly affected the biocatalytic activity of both free and immobilized cellulase. The maximum activity of free cellulase was found at 50 °C; after that, its activity decreased considerably between 50 °C and 70 °C. A significant decline in biocatalytic activity of free cellulase above 50 °C was attributed to the structurally thermal denaturation of cellulase as it was exposed directly to a highly hydrolyzed temperature [36]. Both immobilized cellulase on ZnO(I)-ZEO and immobilized cellulase on ZnO(II)-ZEO showed the best performance at 40 °C, and this was set to be 100% of activity at this maximum hydrolysis temperature. When the hydrolysis temperature was at 30 °C, the immobilized cellulase on ZnO(I)-ZEO and immobilized cellulase on ZnO(II)-ZEO exhibited activities of 85.32% and 67.95%, respectively,

while that of the free cellulase was only 26.89%. This finding demonstrates that, after immobilization, both immobilized cellulases performed well at a low temperature. The decrease in temperature along with an increase in stability of the immobilized cellulase might be due to the modification of the conformational integrity between the molecular structure of the cellulase and the support, making immobilized cellulase suitable to perform at a low temperature with a slight structural change. As depicted in Figure 4 (b), the hydrolysis temperature may be affected not only by the molecular structure of cellulase but also by the surface of the support due to the biocatalytic activity of immobilized cellulase decreasing when the temperature increases. Interestingly, the biocatalytic activity of immobilized cellulase was stable when the temperature was between 50 °C and 60 °C. Finally, when the hydrolysis temperature was 70 °C, the activities were only 23.70% and 25.26% for immobilized cellulase on ZnO(I)-ZEO and immobilized cellulase on ZnO(II)-ZEO, respectively, while free cellulase was only 20.43%. This observation simply demonstrates that immobilized cellulases possess high thermal stability. Improved thermal stability of cellulase after immobilization might be because of the existence of covalent binding between the amino functionalized ZnO-ZEO and cellulase enzyme molecules, thus resulting in conformational stabilization of cellulase on the support.

3.3 Enzyme kinetics study

The efficiency of the cellulase immobilization method on MCC substrate hydrolysis was assessed by investigating the shifts in kinetic parameters. The Michaelis constant (K_m) and maximum velocity (V_{max}) were determined by a Lineweaver-Burk plot, as depicted in Figure 5 and Table 1. The K_m reflects the affinity of the enzyme on the substrate; thus, a lower value of K_m demonstrates that the enzyme displays a significant substrate affinity [9,16]. The K_m value can be changed during enzyme immobilization; this may be due to a modification in activation energy, pH profile, as well as the orientation that existed as a consequence of the immobilization technique [32,37].

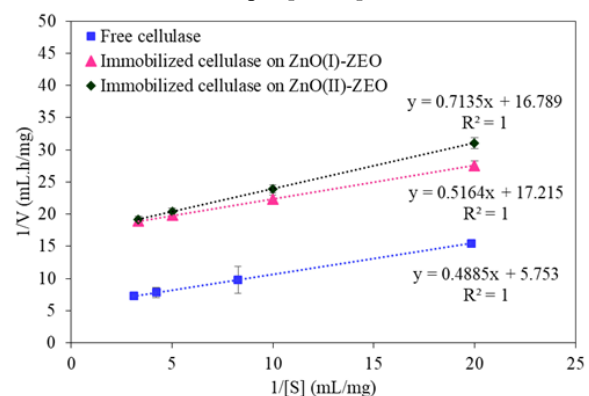


Fig. 5. Lineweaver-Burk plot for immobilized cellulase on ZnO(I)-ZEO, immobilized cellulase on ZnO(II)-ZEO, and free cellulase.

As presented in Table 1, the immobilized cellulase on ZnO(I)-ZEO and immobilized cellulase on ZnO(II)-ZEO showed lower K_m and V_{max} values than those of free cellulase. This finding indicates that the immobilized cellulases were more hydrophilic than free cellulase. Thus, in an aqueous hydrolyzed reaction solution, immobilized cellulase can more easily access the substrate. A decrease in the K_m value indicates significant hydrophilicity of both immobilized cellulases. Moreover, a decline in the V_{max} value was found for immobilized cellulase, which may possibly be due to the decrease in active sites of cellulase and the restriction of cellulase flexibility. Another study also investigated the decrease of both the K_m and V_{max} of immobilized cellulase [9].

Table 1. The kinetic parameters of free and immobilized cellulases

Types of cellulase	Kinetic parameters	
	V_{max} (mg/mL/h)	K_m (mg/mL)
Free cellulase	0.17 ± 0.00	0.09 ± 0.00
Immobilized cellulase on ZnO(I)-ZEO	0.06 ± 0.00	0.03 ± 0.00
Immobilized cellulase on ZnO(II)-ZEO	0.06 ± 0.00	0.04 ± 0.00

3.4 Reusability assay

Free cellulase can only be used once because of its strong reaction with the substrate and difficulty in separation after use. Thus, the aim of immobilization is to enhance stability, reduce production costs, and enable reuse in practical applications. The reusability of immobilized cellulase on ZnO(I)-ZEO and immobilized cellulase on ZnO(II)-ZEO was tested by hydrolyzing MCC at 50 °C for 1 h by keeping a constant pH at 5. Upon completion of each reaction bath, the immobilized cellulases were collected by a simple filtration technique; they were then thoroughly washed with deionized water and reused in the next hydrolysis batch. A total of four cycles was performed to observe the reusability of the immobilized cellulases. As illustrated in Figure 6, the biocatalytic activity of immobilized cellulase on ZnO(I)-ZEO and immobilized cellulase on ZnO(II)-ZEO in the second cycle was 52.56% and 47.38%, respectively. The loss of cellulase biocatalytic activity in the second and subsequent cycles was observed due to the insufficient binding efficiency between the cellulase and the support, thereby causing the cellulase to leach [22,36]. The fourth cycle test for immobilized cellulase on ZnO(I)-ZEO and immobilized cellulase on ZnO(II)-ZEO showed biocatalytic activity of about 19.29% and 10.88%, respectively. In summary, the biocatalytic activity of the immobilized cellulase on ZnO(I)-ZEO and Zn(II)-ZEO reduced up to 80.71% and 89.12%, respectively. The sudden decrease of

biocatalytic activity after the third and fourth hydrolysis cycles may be due to the structural changes of the support in the successive runs and the forceful shaking during each hydrolysis cycle [32].

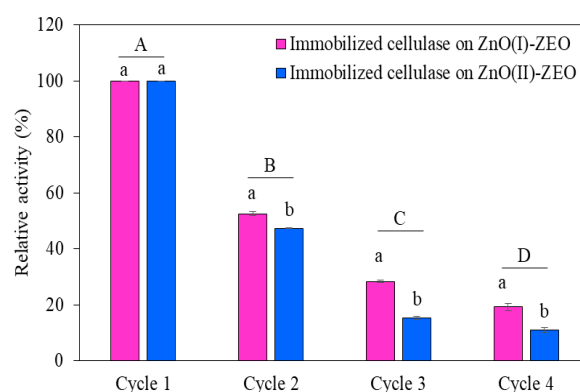


Fig. 6. Reusability and recyclability of immobilized cellulase on ZnO(I)-ZEO and immobilized cellulase on ZnO(II)-ZEO. Note that A, B, C, and D and a and b show significant difference between cycles and samples, respectively ($p < 0.05$; $n = 3$).

3.5 Cumulative yield of reducing sugar

The hydrolysis efficiency of immobilized cellulase on MCC was experimentally compared to free cellulase. Although free cellulase has a strong interaction with a substrate and speedily releases by-products, it is difficult to separate after use. Immobilized cellulase can be used to overcome this drawback. In this work, cellulase immobilized on ZnO(I)-ZEO and ZnO(II)-ZEO could be repeatedly used for as many as four successive runs. As illustrated in Figure 7, a total reducing sugar (TRS) yield of 291.42 ± 1.76 mg/g MCC, 329.57 ± 1.96 mg/g MCC, and 420.96 ± 23.30 mg/g MCC were obtained from the first cycle of MCC hydrolyzed by immobilized cellulase on ZnO(I)-ZEO, immobilized cellulase on ZnO(II)-ZEO, and free cellulase, respectively. The TRS yields obtained from immobilized cellulase on ZnO(I)-ZEO and immobilized cellulase on ZnO(II)-ZEO were 1.44 and 1.28 times lower than the free cellulase. On the other hand, after four cycles, the overall reducing sugar yield obtained from immobilized cellulase on ZnO(I)-ZEO and immobilized cellulase on ZnO(II)-ZEO were 556.61 ± 3.63 mg/g MCC and 552.84 ± 5.14 mg/g MCC, respectively, which were 1.32 and 1.31 times higher than that of free cellulase. Similarly, the cumulative TRS yield obtained from biocatalytic reaction of immobilized cellulase on sodium alginate-polyethylene glycol-chitosan (SA-PEG-CS) was 22.68% higher than that of free cellulase [16]. Therefore, immobilized cellulase can be used as an alternative enzyme for enhanced reducing sugar production.

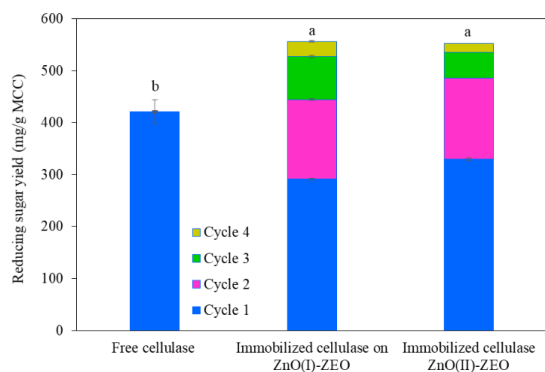


Fig. 7. Results comparing the cumulative reducing sugar yield of enzymatic hydrolysis on MCC. Note that a and b illustrate significant differences between samples ($p < 0.05$; $n = 3$).

4 Conclusion

This study demonstrated a method for the immobilization of cellulase on a ZnO-ZEO support. The successfully immobilized cellulase was confirmed by SEM, XRD, and FTIR. The immobilization efficiencies of the immobilized cellulase on ZnO(I)-ZEO and immobilized cellulase on ZnO(II)-ZEO was $58.17 \pm 0.75\%$ and $55.51 \pm 0.81\%$, respectively. Based on kinetic data, lower values of K_m and V_{max} were observed for the immobilized cellulases, which indicates better hydrophilicity along with a decline in active sites and a reduction of cellulase flexibility after immobilization. Thus, both immobilized cellulases exhibited good performance in the process of simple fermentable sugars production, and can be reused for up to four successive recycle runs.

Acknowledgements

The authors are grateful for the financial support from the King Mongkut's University of Technology North Bangkok and National Science and Technology Development Agency, Thailand. Contract no. Grad 007/2564. XRD and SEM analyses were performed using equipment and facilities in the Scientific Instrument and High Performance Computing Center (SICC), Faculty of Applied Science, KMUTNB. We acknowledge the support of Pranee Preecha of the Department of Industrial Chemistry, Faculty of Applied Science, KMUTNB, who assisted in carrying out the FTIR analysis.

References

1. J.E. Hyeon, S.K. Shin, S.O. Han, Design of nanoscale enzyme complexes based on various scaffolding materials for biomass conversion and immobilization, *Biotechnology journal*, **11**,11 (2016): 1386-1396
2. S. Ariaeenejad, E. Motamedi, G. Hosseini Salekdeh, Stable cellulase immobilized on graphene oxide@CMC-g-poly(AMPS-co-AAm) hydrogel for enhanced enzymatic hydrolysis of lignocellulosic biomass, *Carbohydrate Polymers*, **230** (2020): 115661

3. M. Alexandri, R. Schneider, H. Papapostolou, D. Ladakis, A. Koutinas, J. Venus, Restructuring the conventional sugar beet industry into a novel biorefinery: fractionation and bioconversion of sugar beet pulp into succinic acid and value-added coproducts, *ACS Sustainable Chemistry & Engineering*, **7**,7 (2019): 6569-6579
4. R. Alayoubi, N. Mehmood, E. Husson, A. Kouzayha, M. Tabcheh, L. Chaveriat, C. Sarazin, I. Gosselin, Low temperature ionic liquid pretreatment of lignocellulosic biomass to enhance bioethanol yield, *Renewable Energy*, **145** (2020): 1808-1816
5. Z. Ziaei-Rad, J. Fooladi, M. Pazouki, S.N. Gummedi, Lignocellulosic biomass pre-treatment using low-cost ionic liquid for bioethanol production: An economically viable method for wheat straw fractionation, *Biomass and Bioenergy*, **151** (2021): 106140
6. M. Balat, Production of bioethanol from lignocellulosic materials via the biochemical pathway: A review, *Energy Conversion and Management*, **52**,2 (2011): 858-875
7. A. Limayem, S.C. Ricke, Lignocellulosic biomass for bioethanol production: Current perspectives, potential issues and future prospects, *Progress in Energy and Combustion Science*, **38**,4 (2012): 449-467
8. A. Stark, Ionic liquids in the biorefinery: a critical assessment of their potential, *Energy & Environmental Science*, **4**,1 (2011): 19-32
9. Y. Sui, Y. Cui, G. Xia, X. Peng, G. Yuan, G. Sun, A facile route to preparation of immobilized cellulase on polyurea microspheres for improving catalytic activity and stability, *Process Biochemistry*, **87** (2019): 73-82
10. T. Eom, S. Chaiprapat, B. Charnnok, Enhanced enzymatic hydrolysis and methane production from rubber wood waste using steam explosion, *Journal of Environmental Management*, **235** (2019): 231-239
11. Z. Qiu, G.M. Aita, M.S. Walker, Effect of ionic liquid pretreatment on the chemical composition, structure and enzymatic hydrolysis of energy cane bagasse, *Bioresource Technology*, **117** (2012): 251-256
12. R.H.Y. Chang, J. Jang, K.C.W. Wu, Cellulase immobilized mesoporous silica nanocatalysts for efficient cellulose-to-glucose conversion, *Green Chemistry*, **13**,10 (2011): 2844-2850
13. W. Huang, S. Pan, Y. Li, L. Yu, R. Liu, Immobilization and characterization of cellulase on hydroxy and aldehyde functionalized magnetic Fe_2O_3/Fe_3O_4 nanocomposites prepared via a novel rapid combustion process, *International Journal of Biological Macromolecules*, **162** (2020): 845-852
14. M. Abbaszadeh, P. Hejazi, Metal affinity immobilization of cellulase on Fe_3O_4 nanoparticles with copper as ligand for biocatalytic applications, *Food Chemistry*, **290** (2019): 47-55

15. O.C. Amadi, I.P. Awodiran, A.N. Moneke, T.N. Nwagu, J.E. Egong, G.C. Chukwu, Concurrent production of cellulase, xylanase, pectinase and immobilization by combined Cross-linked enzyme aggregate strategy- advancing tri-enzyme biocatalysis, *Bioresource Technology Reports*, **18** (2022): 101019
16. Y. Wang, C. Feng, R. Guo, Y. Ma, Y. Yuan, Y. Liu, Cellulase immobilized by sodium alginate-polyethylene glycol-chitosan for hydrolysis enhancement of microcrystalline cellulose, *Process Biochemistry*, **107** (2021): 38-47
17. S. Raza, X. Yong, J. Deng, Immobilizing cellulase on multi-layered magnetic hollow particles: Preparation, bio-catalysis and adsorption performances, *Microporous and Mesoporous Materials*, **285** (2019): 112-119
18. B. Qi, J. Luo, Y. Wan, Immobilization of cellulase on a core-shell structured metal-organic framework composites: Better inhibitors tolerance and easier recycling, *Bioresource Technology*, **268** (2018): 577-582
19. E.C. Lau, H.H. Yiu, Chapter 11 - Enzyme immobilization on magnetic nanoparticle supports for enhanced separation and recycling of catalysts, *In Nanomaterials for Biocatalysis*, (2022): 301-321
20. Q. Li, Y. Chen, S. Bai, X. Shao, L. Jiang, Q. Li, Immobilized lipase in bio-based metal-organic frameworks constructed by biomimetic mineralization: A sustainable biocatalyst for biodiesel synthesis, *Colloids and Surfaces B: Biointerfaces*, **188** (2020): 110812
21. D. Zhang, H.E. Hegab, Y. Lvov, L. Dale Snow, J. Palmer, Immobilization of cellulase on a silica gel substrate modified using a 3-APTES self-assembled monolayer, *SpringerPlus*, **5**,1 (2016): 1-20
22. F.R. Paz-Cedeno, J.M. Carceller, S. Iborra, R.K. Donato, A.P. Godoy, A.V. de Paula, R. Monti, A. Corma, F. Masarin, Magnetic graphene oxide as a platform for the immobilization of cellulases and xylanases: Ultrastructural characterization and assessment of lignocellulosic biomass hydrolysis, *Renewable Energy*, **164** (2021): 491-501
23. E. Poorakbar, A. Shafiee, A.A. Saboury, B.L. Rad, K. Khoshnevisan, L. Ma'mani, H. Derakhshankhah, M.R. Ganjali, M. Hosseini, Synthesis of magnetic gold mesoporous silica nanoparticles core shell for cellulase enzyme immobilization: Improvement of enzymatic activity and thermal stability, *Process Biochemistry*, **71** (2018): 92-100
24. M.P. Desai, K.D. Pawar, Immobilization of cellulase on iron tolerant *Pseudomonas stutzeri* biosynthesized photocatalytically active magnetic nanoparticles for increased thermal stability, *Materials Science and Engineering: C*, **106** (2020): 110169
25. M. Zhou, L. Yan, H. Chen, X. Ju, Z. Zhou, L. Li, Development of functionalized metal-organic frameworks immobilized cellulase with enhanced tolerance of aqueous-ionic liquid media for in situ saccharification of bagasse, *Fuel*, **304** (2021): 121484
26. Z. Zhou, X. Ju, M. Zhou, X. Xu, J. Fu, L. Li, An enhanced ionic liquid-tolerant immobilized cellulase system via hydrogel microsphere for improving in situ saccharification of biomass, *Bioresource Technology*, **294** (2019): 122146
27. F. Miao, X. Lu, B. Tao, R. Li, P.K. Chu, Glucose oxidase immobilization platform based on ZnO nanowires supported by silicon nanowires for glucose biosensing, *Microelectronic Engineering*, **149** (2016): 153-158
28. J. Isanapong, P. Pornwongthong, Immobilized laccase on zinc oxide nanoarray for catalytic degradation of tertiary butyl alcohol, *Journal of hazardous materials*, **411** (2021): 125104
29. V. Hooda, A novel polyurethane/nano ZnO matrix for immobilization of chitinolytic enzymes and optical sensing of chitin, *International Journal of Biological Macromolecules*, **106** (2018): 1173-1183
30. R. Batool, S.A. Kazmi, S. Khurshid, M. Saeed, S. Ali, A. Adnan, F. Altaf, A. Hameed, F. Batool, N. Fatima, Postharvest shelf life enhancement of peach fruit treated with glucose oxidase immobilized on ZnO nanoparticles, *Food Chemistry*, **366** (2022): 130591
31. S. Adesoye, K. Dellinger, ZnO and TiO₂ nanostructures for surface-enhanced Raman scattering-based bio-sensing: A review, *Sensing and Bio-Sensing Research*, **37** (2022): 100499
32. N. Antony, S. Balachandran, P.V. Mohanan, Immobilization of diastase alpha-amylase on nano zinc oxide, *Food chemistry*, **211** (2016): 624-630
33. K.N. Rajnish, M.S. Samuel, S. Datta, N. Chandrasekar, R. Balaji, S. Jose, E. Selvarajan, Immobilization of cellulase enzymes on nano and micro-materials for breakdown of cellulose for biofuel production-a narrative review, *International Journal of Biological Macromolecules*, **182** (2021): 1793-1802
34. K. Khoshnevisan, F. Vakhshiteh, M. Barkhi, H. Baharifar, E. Poor-Akbar, N. Zari, H. Stamatis, A.K. Bordbar, Immobilization of cellulase enzyme onto magnetic nanoparticles: Applications and recent advances, *Molecular Catalysis*, **442** (2017): 66-73
35. O. Classics Lowry, N. Rosebrough, A. Farr, R. Randall, Protein measurement with the folin phenol reagent, *Journal of Biological Chemistry*, **193**,1 (1951): 265-75
36. K. Saha, P. Verma, J. Sikder, S. Chakraborty, S. Curcio, Synthesis of chitosan-cellulase nanohybrid and immobilization on alginate beads for hydrolysis of ionic liquid pretreated sugarcane bagasse, *Renewable Energy*, **133** (2019): 66-76
37. D. Tanyolaç, B.I. Yürüksoy, A.R. Özdural, Immobilization of a thermostable α -amylase, Termamyl®, onto nitrocellulose membrane by

Cibacron Blue F3GA dye binding, *Biochemical Engineering Journal*, **2,3** (1998): 179-186